78-801

Technique for Vorticity Measurement in Unsteady Flow

J. E. Keesee,* M. S. Francis,† and J. D. Lang‡
U.S. Air Force Academy, Colo.

A technique is described for determining spatial vorticity distributions in nonstationary fluid flows exhibiting a periodic, time-varying, mean velocity field. The method requires the integration of velocity field data about a spatial array of closed contours to infer the distribution of vorticity using the generalized definition of circulation. A digital data acquisition scheme is suggested for the handling and processing of large quantities of data encountered in typical applications. The method was used to determine the flow characteristics in portions of an unsteady separated region generated by an oscillating spoiler on an airfoil surface. Several data display alternatives are discussed.

I. Introduction

VORTICITY is a significant physical variable in many real fluid flows, but it is a parameter that is often difficult to determine experimentally. The method to be described provides a means of measuring time-varying mean vorticity components and their distributions in nonstationary flows exhibiting a periodic mean velocity field.

Through the years, a number of vorticity measurement techniques have evolved which have been successful to a greater or lesser degree. No single method, however, has proved satisfactory over the entire range of possible flow situations. Attempts to infer the streamwise vorticity component from velocity field measurements date back to the early part of the century.[1] Limitations on velocity measurements techniques at that time did not permit its application to time-varying fluid motions.

A successful method for detecting the freestream-oriented vorticity component was discussed by Kovasznay[2] and Kistler.[3] A special purpose probe was constructed using an array of four hot-wire sensors of equal length and oriented at the same angle with respect to the freestream direction. The four sensors were operated as elements of a single constant current bridge circuit. In addition to the limitation on its directional capability, the wire array size must be of the order of the flow of Kolmogorov microscale for accurate spectral response.[4]

Vane-type mechanical vorticity meters have recently become popular, but these devices are also limited tc measurement of the mean vorticity component in the freestream direction. The first use of these probes was discussed by May.[5] The rotation frequency of the spinner and shaft is converted to an electrical signal using light from a bulb on one side of the shaft. A photocell on the opposite side converts this rotation to a train of pulses whose frequency is a function of the streamwise vorticity component. The resulting spatial resolution is limited by the vane array geometry, while accuracy and linearity are limited by friction in the shaft bearings. Effects of inertia and friction in unsteady flow applications have not yet been documented.

Presented as Paper 78-801 at the AIAA 10th Aerodynamic Testing Conference, San Diego, Calif., April 19-21, 1978; submitted May 22, 1978; revision received Nov. 14, 1978.

Index categories: Nonsteady Aerodynamics; Reseach Facilities and Instrumentation.

*Research Associate, Frank J. Seiler Research Laboratory and Lecturer, Dept. of Aeronautics, Captain USAF. Member AIAA.

†Chief, Mechanics Division, Frank J. Seiler Research Laboratory and Lecturer, Dept. of Aeronautics, Captain USAF. Member AIAA.

‡Associate Professor, Dept. of Aeronautics, Major USAF. Member AIAA.

Although the method that will be described is only capable of inferring the "mean" vorticity component, it is not directionally limited. Its accuracy and reliability in steady flow applications have been discussed previously.[6] In addition, it can be employed to determine a "time-varying mean" value in a nominally periodic unsteady flow. This mean can be extracted, even though the measurement region may exhibit large turbulence intensities.

II. Description of the Method

The technique is based on a simple premise involving no assumptions on the dynamics of the flow under investigation. Its basis stems from the generalized definition of circulation

$$\Gamma(t) = \oint_C U(x,t) \cdot d\ell(x) \tag{1}$$

where Γ is the time-varying circulation about a closed spatial contour C, and $U \cdot d\ell$ is the inner product of the velocity vector with the local path vector on the contour C. Equation (1) can be related to the vorticity variable through Stokes' theorem as follows:

$$\oint_C U(x,t) \cdot d\ell(x) = \int\int_S \xi(x,t) \cdot dS(x) \tag{2}$$

where $\xi = \xi(x,t)$ is the vorticity vector and S is a capping surface of the contour C. If the contour is chosen to lie in a plane (say, the x-y plane) and A is the resulting planar area enclosed by the contour boundaries, the expression for the spatially averaged ($\langle\ \rangle$) component of vorticity orthogonal to the measurement plane can be expressed as:

$$\langle \xi_z(t) \rangle = \frac{1}{A} \oint_C U(x,y,t) \cdot d\ell(x,y) \tag{3}$$

The measurement of any desired component of vorticity can therefore be accomplished by proper orientation of the measurement plane, assuming that the integrand can be evaluated at a representative number of points on the contour boundary. The resolution of the spatial vorticity average is obviously dependent on the size of the contour.

If a number of contours are arranged in an aggregate, the distribution of vorticity in the enclosed region can be inferred. Again, the only restriction on the size of each element of the mesh is that a sufficient number of measurement points occur on each element of the mesh. This condition is limited by such things as the velocity measurement volume (probe volume) and the resolution and accuracy of position measurement. The subsequent resolution of vorticity is directly related to the mesh size of the contour array.

Since Eq. (3) is a result of kinematic conditions, the contour C can take any shape. In practice, it is convenient to choose a contour geometry that is related to the flow being investigated or the experimental apparatus being employed. The remainder of this discussion assumes that the contour array geometry is a planar aggregate of equally sized rectangular elements in the x-y plane.

The spatially averaged z component of vorticity for the ith element of the mesh can then be determined as:

$$\langle \xi_z(t) \rangle_i = \frac{1}{A_i} \oint_{C_i} U(x,y,t) \cdot d\ell(x,y) \tag{4}$$

Similar expressions for the other vorticity components can be obtained by orthogonal rotation of the integration plane.

The extension of these concepts to many real laboratory flows involves the elimination of random fluctuations caused by turbulence and noise. In steady flows this can be accomplished by simple pointwise time averaging of the velocity component signal. If the flow variables are further characterized by a periodic time-varying mean value for any variable q, we can write

$$q(t) = \overline{q(t)} + q'(t) \tag{5}$$

where $\bar{q}$ denotes the time-varying mean value of the variable, and q' is a random fluctuation characterized by the relation:

$$\overline{q'} = 0$$

The mean value of the variable is tied to some large-scale organized structure in the flow which is periodic in nature. It may even be related to a disturbance that drives the flow, e.g., a vibrating surface or other mechanically induced oscillation. The fluctuating quantity is related to turbulence or noise generated within the flow or in the transducer system which seeks to characterize the variable.

The time-varying mean value of the variable must then be extracted by an ensemble averaging or phase-locked averaging technique. If this is accomplished properly, Eq. (4) can be rewritten

$$\langle \overline{\xi_z(t)} \rangle_i = \frac{1}{A_i} \oint_{C_i} \overline{U(x,t)} \cdot d\ell(x) \tag{6}$$

where the overbar denotes the ensemble averaged time-varying mean value of the variable.

The concept of ensemble average is more clearly understood if one considers the time history of the variable being examined. Figure 1a shows the instantaneous history of a variable q over a cycle of motion. The signal characterizing the variable is synchronized to (triggered by) an event which is periodic and repeatable from cycle to cycle. Using a number of these records, each triggered at the same phase point, data at common phase points are added together to form an ensemble average at that point. All phase points can then be recombined to provide the average time history (Fig. 1b). The number of records necessary for an adequate average depends on a number of factors, including the local intensity of the random fluctuations. The number of operations required for this type of averaging can be very large for manual calculation, but is not a difficult task for a digital computer.

A comment should now be made concerning possible methods for obtaining simultaneous position and velocity field measurements. Examination of the preceding equations indicates that the desired velocity component is the one tangential to the contour segment under examination. Therefore, a velocity measurement technique capable of resolving at least two components is necessary. In addition, to be useful in nonstationary flows, the transducer must have a frequency response at least as high as the highest harmonics found in the mean motion. Finally, the measurement system must be capable of locating the velocity measurement volume at all points on the contour or contour array while simultaneously assessing its instantaneous position. At present, a continuously positionable multicomponent hot-wire anemometry probe or a laser Doppler velocimeter (LDV) with a traversable measurement volume are two possible instruments having the desired attributes and amenable to application in a wide range of experimental situations. The hot-wire technique is less expensive and simpler to implement than the LDV, but cannot be used readily in reversing flows or flows exhibiting high turbulence levels. The probe geometry can be selected for the particular application. The LDV system may require flow seeding but provides a nonintrusive flow measurement technique for use in many highly complex flowfield geometries.

The successful implementation of this technique requires an accurate evaluation of Eq. (6) over a large number of points in space and time. To manage and manipulate these data, a digital computer of some sort is a necessity in all but the most trivial of problems. If we restrict ourselves to the determination of only a single (z) component of vorticity over a predetermined mesh of equal size rectangular contours in the x-y plane, Eq. (6) can be rewritten as:

$$\langle \overline{\xi_z(\phi)} \rangle_{ij} = \langle \overline{\xi_z(x_i,y_j,\phi)} \rangle = K \oint_{C_{ij}} \overline{U(x,y,\phi)} \cdot d\ell(x,y) \tag{7}$$

where x_i and y_j are the spatial coordinates of the center of the mesh element C_{ij}, that is, the contour centered on row i and column j of the array; K is a constant representing the inverse of the mesh size (averaging area) $1/A$; and ϕ is the periodic drive phase angle (a dimensionless formulation of time). The spatial average over element C_{ij} is ascribed to be valid at the point (x_i,y_j). Each contour segment is represented by an equally spaced aggregate of data sampling locations. As the probe (velocity transducer) moves to a new location, it must be programmed to select the appropriate component for that contour segment. The ensemble averaged sum of the ℓth velocity component over n records can then be written

$$\overline{U_\ell(x,y,\phi_\alpha)} = \frac{1}{n} \sum_{k=1}^{n} U_{\ell_k}(x,y,\phi_\alpha) \tag{8}$$

where an individual record is denoted by the additional subscript k. The subscript α on the phase angle variable represents the digital sampling phase point. The total number of temporal sampling points is determined by the desired resolution over the sampling period, which, in turn, must be related to the highest frequencies encountered in the local mean value of the variable waveform and is limited by the maximum sample rate of the data acquisition system.

The resulting ensemble averaged record is now stored for subsequent use with records from the other spatial data locations. If all elements of the mesh are geometrically similar and the same size, say, having segment lengths of Δx and Δy aligned in the x and y directions, respectively, then the integral equation giving the vorticity value for the element C_{ij} can be written:

$$\begin{aligned}\langle \overline{\xi_z(\phi_\alpha)} \rangle_{ij} = K\Bigg\{ &\int_{x_i-(\Delta x/2)}^{x_i+(\Delta x/2)} \overline{U_x\left(x,y_i+\frac{\Delta y}{2},\phi_\alpha\right)}\, dx \\ &+ \int_{y_i+(\Delta y/2)}^{y_i-(\Delta y/2)} \overline{U_y\left(x_i+\frac{\Delta x}{2},y,\phi_\alpha\right)}\, dy \\ &+ \int_{x_i+(\Delta x/2)}^{x_i-(\Delta x/2)} \overline{U_x\left(x,y_i-\frac{\Delta y}{2},\phi_\alpha\right)}\, dx \\ &+ \int_{y_i-(\Delta y/2)}^{y_i+(\Delta y/2)} \overline{U_y\left(x_i-\frac{\Delta x}{2},y,\phi_\alpha\right)}\, dy \Bigg\}\end{aligned} \tag{9}$$

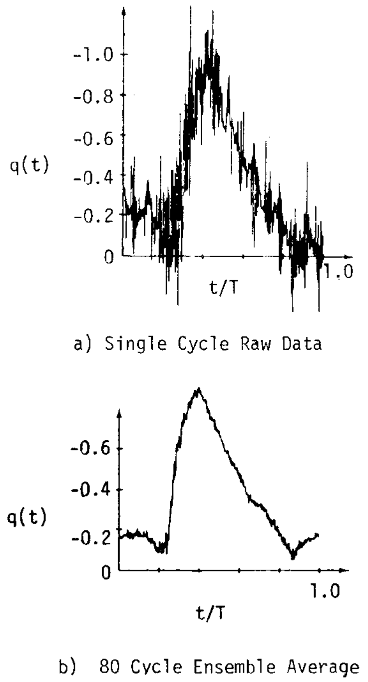

Fig. 1 Comparison of instantaneous data with corresponding ensemble average.

These integrals can be performed subsequent to the data acquisition process. Depending on the number of data points used to define each contour segment, several digital integration schemes are available. When a small number of points are involved, a trapezoidal rule integration technique may be employed. If more sampling locations are used to represent a contour segment, greater accuracy can be derived using Simpson's rule.

III. Application to an Unsteady Separated Flow

Description of the Experiment

To demonstrate the usefulness of the method, results are presented from an experiment involving an unsteady separated flow. The separation zone was generated on a symmetric (NACA 0012) airfoil behind a sinusoidally oscillating fence-type spoiler located at midchord on one surface. The experiment was conducted in the USAF Academy 0.61×0.91 m (2×3 ft) subsonic wind tunnel. All measurements were obtained at undisturbed freestream speeds low enough for the flow to be construed as incompressible. The spoiler oscillation frequency could be fixed at values up to 30 Hz. Spoiler mean height and amplitude could also be adjusted for a given series of measurements.

A multicomponent constant temperature, linearized hot-film anemometry system was employed for velocity field measurements in the region surrounding the reverse flow portion of the separation zone. An X-geometry hot-film probe was oriented to provide two orthogonal components of velocity in the integration (x,y) plane. Analog output voltages, which were directly proportional to the instantaneous velocity component magnitudes, were then sampled by a Digital Equipment Corp. PDP 11/45 data acquisition system.

A triggering mechanism composed of a small light source and photocell combination was attached to the spoiler drive unit to provide a pulsed output which corresponded to a prescribed (usually minimum) value of the spoiler height. Using this output as a trigger source had the effect of providing a phase-lock on the initiation of data sampling to an event directly related to the periodic flowfield drive.

The probe was moved and accurately positioned by a motorized three-dimensional traversing mechanism employing orthogonal ball bearing screw drive assemblies. Continuous analog position outputs were available from multiturn precision potentiometers appropriately geared to the drive assemblies. A simple amplifier circuit was used to convert the instantaneous resistance ratio of each potentiometer to a voltage proportional to location. The miniature dc drive motors were powered through an amplifier actuated by an output voltage from digital-to-analog converter interfaced with the PDP 11/45 system or other suitable voltage source for manual control.

A general schematic of the experimental apparatus is presented in Fig. 2.

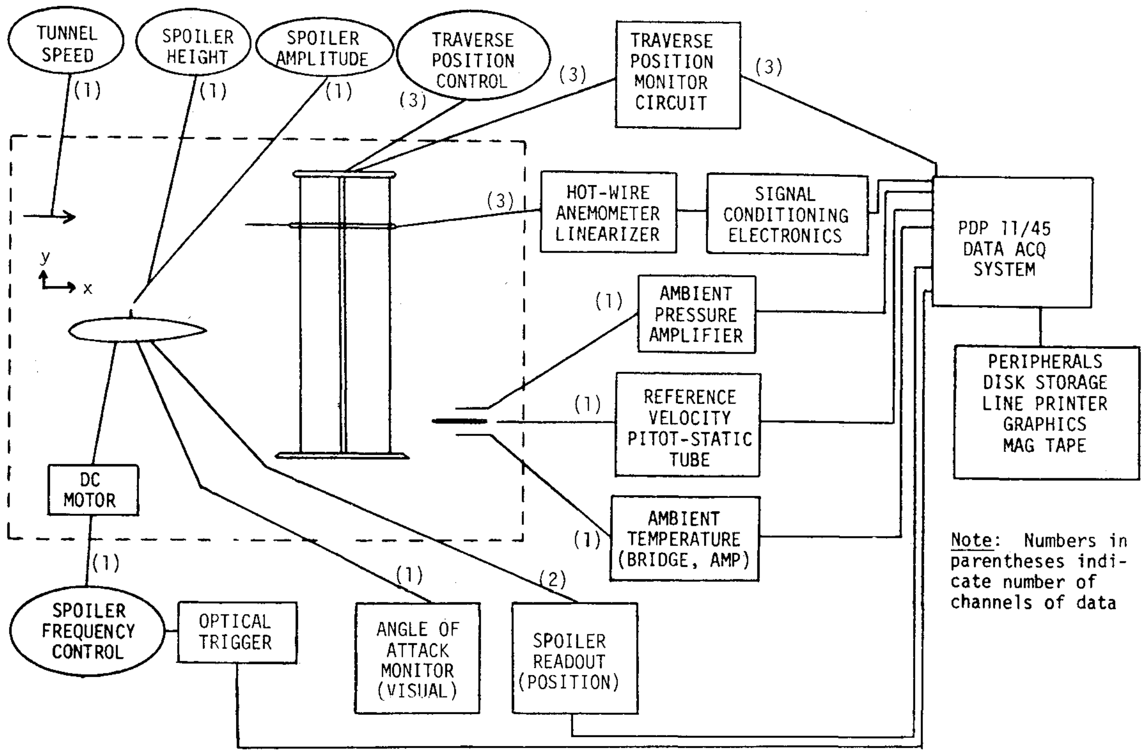

Fig. 2 Schematic of experimental apparatus.

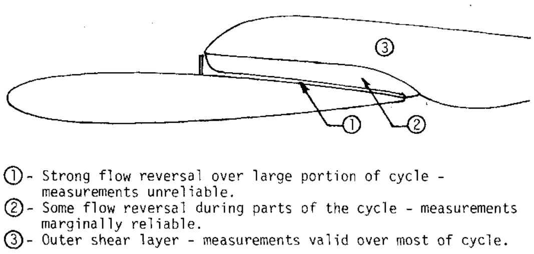

Fig. 3 Reliability of hot-wire measurements in the vorticity bearing region (typical).

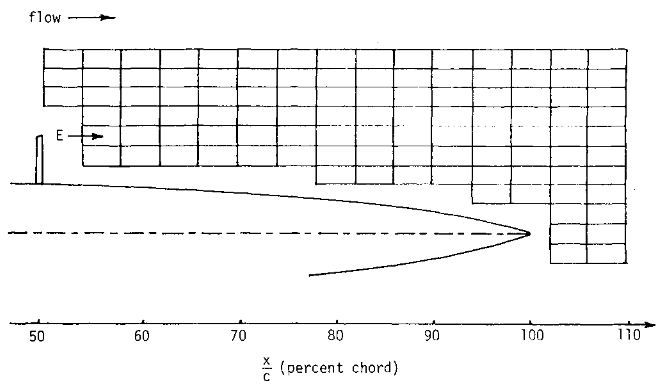

Fig. 4 Contour array geometry.

The use of hot-film anemometer probes presented certain limitations on the possible measurement locations due to the intermittent reversing nature of the flow. Data validation was, therefore, accomplished using both analog comparator circuits and a software verification scheme in conjunction with flow visualization photographs.

An additional concern related to the geometry of the two-wire probe was the potential error introduced by an out-of-plane velocity component on the linearized anemometry system. This effect has been neglected here due to the two-dimensional nature of the experimental configuration. This assumption is considered reasonable in view of the results of calculations previously published by Francis et al.,[6] who showed that these errors are small for small values of the out-of-planeness angle.

Flow reversal was found to be most pronounced near the airfoil surface with an almost dead-air region immediately behind the spoiler and extending downstream (Fig. 3). The hot-film technique was thought to be applicable in the outer shear layer region and a portion of the dead-air zone. To further insure that only valid data were being collected, data locations where the local x component of velocity did not exceed 25% of the freestream value were so designated. In addition, an analog circuit was constructed which compared the instantaneous downwash angle, $\theta(U_y/U_x=\tan\theta)$, to a preset threshold well within the limits of the wire array geometry. If an inordinate amount of data were found to exceed this value, the sampling location was not used.

Selection of the contour array geometry was based on a number of factors, including the probe measurement volume, the location and size of the separated region and shear layer, and desired resolution of the vorticity field. A schematic of the rectangular mesh used is shown in Fig. 4. In this case, a total of 390 sampling locations were employed. The value of the integral for each rectangular element of the mesh was determined using ten values of the velocity field at six spatial locations.

Data Acquisition Sequence and Program

The data acquisition and reduction algorithm involved the conversion of hot-film signal voltage to velocity, appropriate testing for data validity (flow angle and magnitude), ensemble averaging as just discussed, and subsequent storage of the averaged data on disk. Each data set was tagged with the probe location and aerodynamic reference data (pressure, temperature, freestream velocity, etc.). Upon completion of the storage of each data set, program control was exercised to reposition the probe through a D/A converter voltage output. The data acquisition and repositioning process was accomplished until the entire contour sequence was completed. A diagram of the algorithm is provided in Fig. 5. Upon completion of the experiment, disk-stored average data were recalled to core memory for the spatial integration calculations. Individual data points were integrated to provide the circulation of various mesh elements at discrete phase points as described previously. Repetition of the integration procedure for other phase angles then provided the entire spatial and temporal distributions.

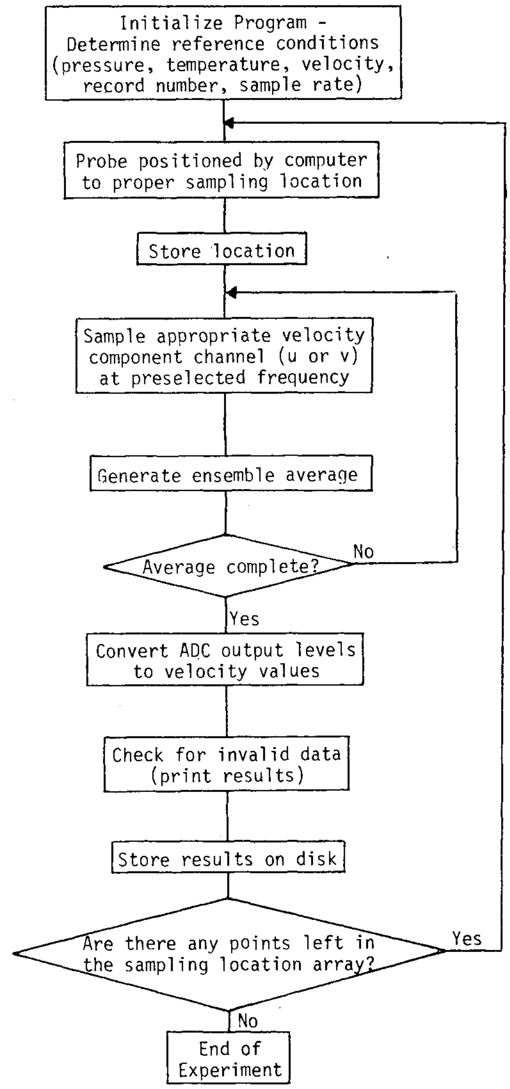

Fig. 5 Program flowchart.

The heart of the data acquisition program is a real-time synchronous analog-to-digital conversion subroutine whereby up to 24 analog input channels can be alternately read at an overall sample rate of up to 2.5 kHz. The actual data acquisition rate was chosen on the basis of the spoiler frequency. On the basis of preliminary velocity field measurements, it was determined that between 80 and 160 data points would properly represent a cycle of data. An algorithm was therefore developed to reduce the sample rate as the spoiler frequency was decreased, which served to maintain the quantity of samples within the desired limits of cycle representation while sampling at frequencies which were integer multiples of the computer clock frequency.

Program execution was initiated by the acquisition and storage of required reference variable values. The data and time of test were automatically noted by the computer system. The user was then queried by the system to provide the spoiler oscillation frequency, amplitude and mean height, and the number of cycles to be used for each ensemble average. Ambient static pressure and temperature (p_∞ and T_∞, respectively) were provided by sensors whose output was coupled to the data acquisition system. The freestream velocity was calculated from the output of a pressure transducer connected to a pitot-static system. The measurement was made with the spoiler retracted (steady flow conditions). These data were employed to calibrate and scale subsequent hot-film measurements.

The spatial position of the probe could be optionally controlled through program software. A file stored on disk contained predetermined coordinates ordered sequentially. The number and location of these coordinates was, of course, determined by the nature of the spatial contour array geometry. Probe positioning was effected through a subroutine in which the instantaneous position was compared with the desired location. This comparison was made during probe movements approximately once every millisecond. For each coordinate direction, the polarity of the algebraic difference in these two numbers was used to select the appropriate motor drive direction. As this difference was decreased toward zero, the drive voltage was also reduced until the requisite location was attained. The test to insure a position match required the difference to be less than or equal to 0.12 mm. Upon completion of the relocation process, a flag was set signaling the initiation of the velocity data acquisition sequence.

Sampling was accomplished for approximately one and one-half spoiler oscillations to allow for an evaluation of repeatability and to allow the computer time to perform its required calculations before the next cycle began. Triggering from the output pulse of the optical pickup insured that each record was initiated at the same phase point. The computer therefore sampled during two spoiler cycles for each full record of data to be averaged.

The appropriate velocity component, that is, the one tangential to the local contour segment direction, was predetermined for each location. Velocity component magnitudes at a given phase point were summed with corresponding values from the remaining records in the ensemble. The resulting sum was divided by an integer representing the total number of records. The resulting record representing the average was then written on disk.

The repositioning and acquisition sequence was repeated through the entire array of spatial locations. Upon completion of these measurements, the spoiler was retracted and the reference variables remeasured to calculate the total drift in the electronic systems and the ambient freestream conditions. Drift problems posed a major source of possible error due to the extensive measurement time intervals encountered. This problem can be more fully appreciated by realizing that although only 72,000 or so words of data were stored on disk for a given experimental situation, approximately 1.8×10^6 data words were processed through the computer CPU during a typical experiment. An approximation for the overall time interval, T_M, is given by the relation:

$$T_M = (Q+1)t_l + QNt_2 \tag{10}$$

where:

$t_2 = 1/f_s \cdot$ integer part of $[2.0 + t_c \cdot f_s]$
t_c = computation time
Q = number of spatial sampling locations
N = number of records per average
f_s = spoiler oscillation frequency
t_l = typical traversal time from one spatial location to the next

At high oscillation rates, t_2 was observed to extend to three spoiler periods because of the computation time. At frequencies below 15 Hz, it remained at two spoiler periods. t_l was found to average approximately 4 s. Table 1 shows a comparison of typical measurement time intervals as a function of spoiler oscillation frequency for the contour array shown in Fig. 4.

It is observed that exceptionally low values of spoiler frequency can result in prohibitive measurement periods. Therefore, the selection of the contour array geometry must be based, in part, on the attainment of a reasonable experimental time interval.

Table 1 Comparison of measurement time intervals

$T_M = (Q+1)t_l + (QN/f_s) \cdot \mathrm{Int}[2.0 + t_c \cdot f_s]$[a]

f_s(Hz)	T_M
20	42.3 min
10	58.6 min
5	1.52 h
1	5.85 h
0.5	11.3 h
0.1	2.28 days
0.05	4.53 days
0.01	22.6 days

[a] $Q = 390$ (sample points), $N = 25$ (records), $t_l = 4$ s (approximately).

Sources of Error

Integration is fundamentally a smoothing process. Any increased accuracy achieved through the use of this technique is, however, countered by a decrease in spatial resolution. This must be a consideration in the selection of the fundamental contour grid element size.

The number of points used to define each contour directly affects the type of digital integration scheme which might be used and hence affects the accuracy. The actual effect of the integration scheme is difficult to evaluate, since it is determined to a great extent by the nature of the local velocity gradient which is time dependent. A scheme employing the trapezoidal rule approximation was selected in the present case due to the close proximity of measurement locations compared to typical velocity gradients (determined from preliminary measurements) and the desired spatial resolution.

Errors in computation of the ensemble average can arise from inaccuracies in temporal sampling intervals. This source of error is primarily dependent on data acquisition system characteristics, especially clock frequency errors. Most commerical systems, including the one just discussed, provide more than adequate performance for this type of application.

The principal sources of measurement error in the present experiment arise from two sources—velocity measurement errors and probe positioning error.

The use of the hot-wire anemometer for velocity measurement presents certain inaccuracies which have been discussed by numerous previous investigators, for example, Refs. 7 and 8. Its limitations are a primary reason that the examples discussed in the present paper are spatially restricted to the outer shear layer.

Probe positioning error was ultimately determined by the overall accuracy of the traversal system and the resolution of the analog-to-digital converter, which was used to provide the computer with an instantaneous indication of position.

An accurate expression describing the measurement error is difficult to establish since it must depend on instantaneous values of the local velocity gradients. However, an ap-

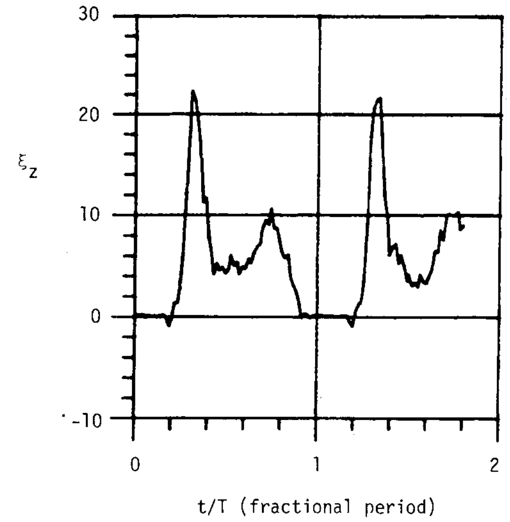

Fig. 6 Average nondimensional vorticity ($\xi = \omega c / 2U_\infty$) time history, contour E, frequency = 19.4 Hz, U_∞ = 18.4 m/s.

proximation providing an estimate of the error due to the combined effects of velocity and position inaccuracies can be determined for a rectangular contour of sides ℓ_x and $\ell_y = k_1 \ell_x$. If the flow is characterized by a typical velocity having components U_x and $U_y = k_2 U_x$, the magnitude of the error can be expressed as:

$$E_\xi = \frac{E_u}{k_1} \frac{(1+k_1^2)}{(1+k_1 k_2)} + \left(\frac{\Delta U_x}{U_x}\right)\left(\frac{\ell'}{\ell_x}\right) \frac{(1+k_1^2 k_2)}{k_1(1+k_1 k_2)} \qquad (11)$$

where E_u is the error in velocity measurement expressed as a percentage; ΔU_x is the typical difference in mainstream velocity across the contour; and ℓ' is the resolution/accuracy of the position measurement system.

A worst-case value for the error for a typical contour employed in the present experiment is approximately 2.5%.

IV. Some Experimental Results

Suitable interpretation and display of the data obtained using the contour integration technique can provide a means of observing the generation of vorticity filaments and their subsequent motion in space and time.

The initial result of a single contour integration provides a description of the average vorticity at a single point as a function of time. Figure 6 shows a typical variation of this parameter. These results were obtained for the contour grid element labeled "E" in Fig. 4 (just aft of the spoiler) and represents a 25-record average. The number of records employed to determine the average was selected after tests were conducted for 25, 50, and 100 record size ensembles at several characteristic spatial locations. The results of these tests showed marked convergence to the mean using only a few records. The low-level fluctuations retained with a 25-record ensemble did not appear to influence the characterization of the mean flow significantly. The use of a 25-record average also resulted in minimal run times over which stable control of the dynamic and environmental variables could be maintained.

As expected, the average vorticity exhibits a period corresponding to the spoiler drive value, but the signal in no way resembles the input sinusoid. Repeatability of the average value is verified by comparing the curve shape characteristics of the two different cycles shown in Fig. 6. This characteristic is somewhat compromised at phase points where the local flow is excessively turbulent. The apparent fluctuations can be removed by increasing the averaging record size, thereby increasing the total test time, or by an a posteriori curve-smoothing technique.

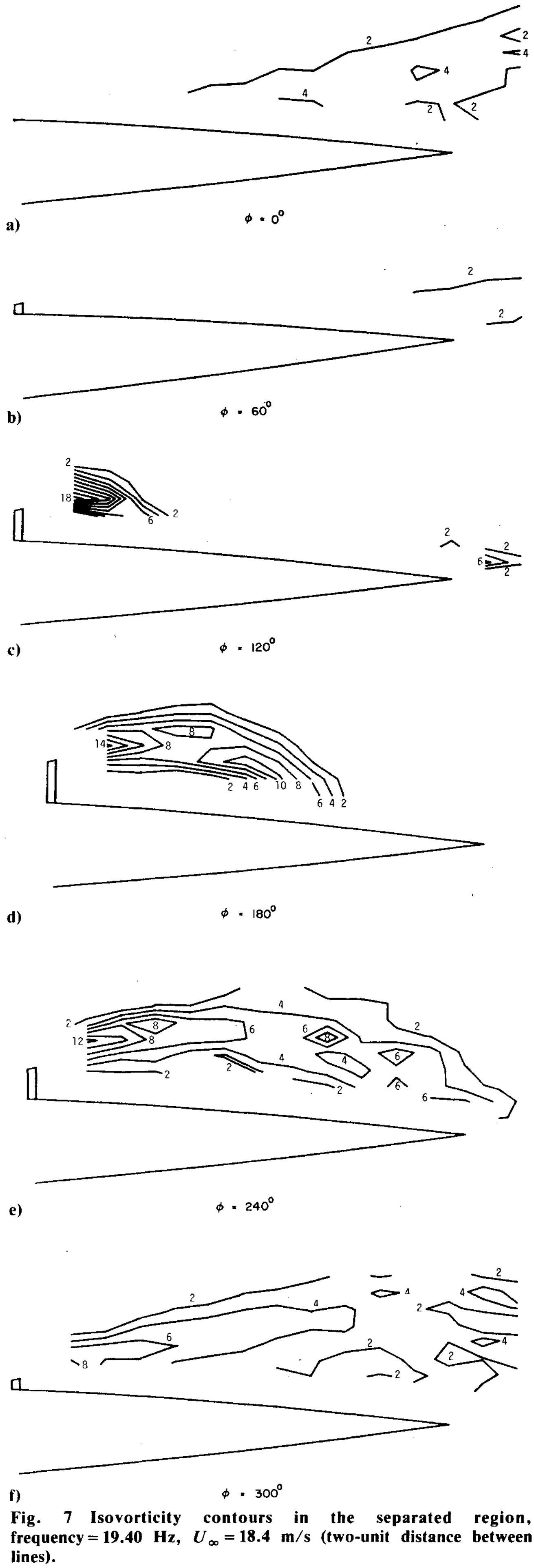

Fig. 7 Isovorticity contours in the separated region, frequency = 19.40 Hz, U_∞ = 18.4 m/s (two-unit distance between lines).

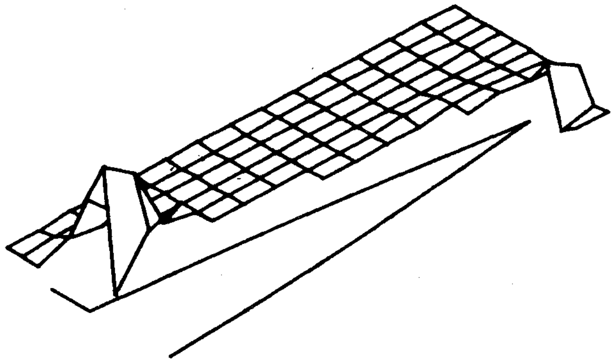

Fig. 8 Perspective sketch of vorticity field, $\phi = 120$ deg, frequency = 19.40 Hz, $U_\infty = 18.4$ m/s.

An examination of the results reveals the existence of a time delay in the appearance of vorticity within the contour. The character of the vorticity field is observed to change as fluid passes through the region followed by the total transfer of all rotational effects from the contour enclosed area near the end of the cycle.

The key to reconstructing the global motion of the vorticity field rests on the suitable cross plotting of these data with spatial position. First, a phase angle is selected for the desired display; that is, one would like to display the spatial distribution of vorticity at a given instant of time, or phase angle. This procedure is not difficult to accomplish if the vorticity time histories at individual points are properly tagged with the representative spatial location.

While it is comparatively easy to generate graphs of the vorticity variable with either the cross-stream or downstream directions, it is difficult to visualize fully the three-dimensional nature of the data from this perspective. A more informative two-dimensional representation can be provided by constructing a contour map that depicts lines of constant vorticity, or isovorticity contours. This has been done in Fig. 7 for a given set of flow conditions in which six phase points have been selected to illustrate the evolution of the distribution of vorticity over a cycle of spoiler motion. Isovorticity contours are projected into the X-Y plane (physical space) at equal intervals. The wing location and instantaneous spoiler position have been sketched into the figures to provide a realistic geometric reference. The convection and diffusion of vorticity packets are more easily tracked in this format than with a series of more conventional two-dimensional graphs.

In this example, the data were obtained at a relatively high oscillation frequency to illustrate more clearly some of the phase lags which might be encountered from true unsteady effects. Although regions of negative vorticity were found to exist near the trailing edge, only those zones where positive (clockwise rotation) vorticity exists have been displayed to prevent even more crowding of data in these figures.

At most spoiler heights on the upstroke (0 deg $< \phi <$ 90 deg), one observes vorticity generated during the previous cycle wash off the wing surface. At spoiler heights near the maximum value, a tightly wound, more organized structure is formed near the tip of the spoiler. As the spoiler retracts, this vorticity begins to diffuse while simultaneously being convected downstream. The diffusion process is apparent from observation of the redistribution of vorticity. Both diffusion and convection rates may be expressed in nondimensional form by referencing them to the phase angle.

For some applications, the isovorticity contour representation technique may be more than adequate to visualize the evolution of the vorticity fields, but in some cases, it might be useful to view this distribution as a deforming three-dimensional surface. A perspective view of such a surface is provided in Fig. 8 in which the observer is allowed to examine the surface at an angle from which he can more fully appreciate the significance of spatial derivatives of the vorticity field without the knowledge of precise values.

V. Summary

Results obtained to date indicate the capability of the method to accurately determine the vorticity distribution in a complex, unsteady flow. A major advantage of the technique is its ability to assess the average vorticity within a region without requiring measurements within it. The spatial resolution of resultant distributions is dictated by the minimum size of the individual contours which are employed. This factor is, in turn, often dictated as much by the capabilities of the available data acquisition system as by the nature of the experimental conditions.

Acknowledgments

This research was sponsored by the Frank J. Seiler Research Laboratory under work unit 2307-F1-34. The authors wish to acknowledge the assistance of C. Geddes, who fabricated the experimental apparatus discussed in this paper.

References

[1]Fage, A. and Simmons, L.F.G., "An Investigation of the Airflow Pattern in the Wake of an Aerofoil of Finite Span," *Philosophical Transactions of Royal Society* (London), Series A, Vol. 225, No. 7, 1925, pp. 303-330.

[2]Kovasznay, L.S.G., "Methods to Distinguish Between Laminar and Turbulent Flow," *High Speed Aerodynamics and Jet Propulsion*, Vol. 9, Princeton, 1954, pp. 213-285.

[3]Kistler, A. L., M.S. Thesis, Johns Hopkins University, 1952.

[4]Wyngaard, J. C., "Spatial Resolution of the Vorticity Meter and Other Hot-Wire Arrays," *Journal of Physics, E*, Vol. 2, 1969, pp. 983-987.

[5]May, D. M., "The Development of a Vortex Meter," M.S. Thesis, The Pennsylvania State University, 1964.

[6]Francis, M. S., Kennedy, D. A., and Butler, G. A., "A Technique for the Measurement of Spatial Vorticity Distributions," *Review of Scientific Instruments*, Vol. 49, May 1978, pp. 617-623.

[7]Comte-Bellot, G., "Hot-Wire Anemometry," *Annual Review of the Fluid Mechanics*, Vol. 8, 1976, pp. 209-231.

[8]Freymuth, P., "Noise in Hot-Wire Anemometers," *Review of Scientific Instruments*, Vol. 39, April 1968, pp. 550-557.